Macromolecules **1995**, *28*, 4116 – 4121; e) C.-M. Lee, A. C. Griffin, *Macromol. Symp.* **1997**, *117*, 281 – 290.
[5] a) R. P. Sijbesma, F. H. Beijer, L. Brunsveld, B. J. B. Folmer, J. H. K. K. Hirschberg, R. F. M. Lange, J. K. L. Lowe, E. W. Meijer, *Science* **1997**, *278*, 1601 – 1604; b) B. J. B. Folmer, E. Cavini, R. P. Sijbesma, E. W. Meijer, *Chem. Commun.* **1998**, 1847 – 1848; c) B. J. B. Folmer, R. P. Sijbesma, E. W. Meijer, *Polym. Mater. Sci. Eng.* **1999**, *80*, 20 – 21; d) J. H. K. K. Hirschberg, F. H. Beijer, H. A. van Aert, P. C. M. M. Magusin, R. P. Sijbesma, E. W. Meijer, *Macromolecules* **1999**, *32*, 2696 – 2705.
[6] a) N. Yamaguchi, D. S. Nagvekar, H. W. Gibson, *Angew. Chem.* **1998**, *110*, 2518 – 2520; *Angew. Chem. Int. Ed.* **1998**, *37*, 2361 – 2364; b) N. Yamaguchi, H. W. Gibson, *Angew. Chem.* **1999**, *111*, 195 – 199; *Angew. Chem. Int. Ed.* **1999**, *38*, 143 – 147.
[7] DMSO, DMF, and methanol all disrupt assembly to form polycaps.
[8] Guest-dependent, liquid crystallinity has been described for molecular clips: J. L. M. van Nunen, B. F. B. Folmer, R. J. M. Nolte, *J. Am. Chem. Soc.* **1997**, *119*, 283 – 291.
[9] Details of the increased viscosity with higher concentration of **1a** in chloroform will be published elsewhere.
[10] Concentration experiments were performed by weighing **1a** into glass capillaries, adding chloroform, flame-sealing, and reweighing. Samples below 36% by weight were isotropic.
[11] S. L. Kwolek, P. W. Morgan, J. R. Schaefgen, L. W. Gulrich, *Macromolecules* **1977**, *10*, 1390 – 1396.
[12] F. D. Saeva, *Liquid Crystals: The Fourth State of Matter*, M. Dekker, New York, **1979**.
[13] C. Ober, J.-I. Jin, R. W. Lenz, *Makromol. Chem. Rapid Commun.* **1983**, *4*, 49 – 51.
[14] Both chloroform and *p*-difluorobenzene are good guests for the polycaps.[2]
[15] At lower concentrations (ca. 38% by weight) the diffraction pattern is much less distinct.
[16] Modeling was performed using MacroModel v.5.5 and the MM2* force-field: F. Mohamadi, N. G. J. Richards, W. C. Guidia, R. Liskamp, C. Caulfield, G. Chang, T. Hendrickson, W. C. Still, *J. Comput. Chem.* **1990**, *11*, 440 – 467.
[17] a) R. W. Lenz, *Pure Appl. Chem.* **1985**, *57*, 977 – 984; b) J. M. Seddon in *Handbook of Liquid Crystals*, *Vol. 1*, *Fundamentals* (Eds.: D. Demus, J. W. Goodby, G. W. Gray, H. W. Spiess, V. Vill), WILEY-VCH, Weinheim, **1998**, pp. 635 – 679.
[18] Freeze-fracture electron microscopy is a common technique for analyzing organic molecules that form gels: a) C. S. Snijder, J. C. de Jong, A. Meetsma, F. van Bolhuis, B. L. Feringa, *Chem. Eur. J.* **1995**, *1*, 594 – 597; b) P. Terech, R. G. Weiss, *Chem. Rev.* **1997**, *97*, 3133 – 3159.
[19] The ^{1}H NMR spectrum of **1a** also indicates intramolecular hydrogen bonding. The resonance attributed to the amide proton appears at $\delta =$ 8.5 – 9.0 in all solvents tested and is concentration independent.
[20] Formation of hydrogen bonds in polymers has been shown to rigidify their structure and cause them to form liquid crystalline phases; see a) T. Kato, J. M. J. Fréchet, *Macromol. Symp.* **1995**, *98*, 311 – 326, and references therein; b) T. Kato, *Supramol. Sci.* **1996**, *3*, 53 – 59, and references therein; c) T. Kato, *Handbook of Liquid Crystals*, *Vol. 2b*, *Low Molecular Weight Liquid Crystals II* (Eds.: D. Demus, J. W. Goodby, G. W. Gray, H. W. Speiss, V. Vill), WILEY-VCH, Weinheim, **1998**, pp. 969 – 979.
[21] P. J. Collings, *Liquid Crystals*, *Nature's Delicate Phase of Matter*, Princeton University Press, Princeton, **1990**.
[22] a) S. C. Simmens, J. W. S. Hearle, *J. Polym. Sci. Polym. Phys. Ed.* **1980**, *18*, 871 – 876; b) K. K. Chawla, *Fibrous Materials*, Cambridge University Press, Cambridge, **1998**, pp. 79 – 95.
[23] A. H. Simmons, C. A. Michal, L. W. Jelinski, *Science* **1996**, *271*, 84 – 87.
[24] For example, see a) C. M. Paleos, D. Tsiourvas, *Angew. Chem.* **1995**, *34*, 1839 – 1855; *Angew. Chem. Int. Ed. Engl.* **1995**, *34*, 1696 – 1711; b) V. V. Tsukruk, *Prog. Polym. Sci.* **1997**, *22*, 247 – 311.
[25] a) G. M. Whitesides, J. P. Mathias, C. T. Seto, *Science*, **1991**, *254*, 1312 – 1319; b) J.-M. Lehn, *Supramolecular Chemistry*, VCH, Weinheim, **1995**; c) M. Muthukumar, C. K. Ober, E. L. Thomas, *Science* **1997**, *277*, 1225 – 1232.
[26] a) M. M. Conn, J. Rebek, Jr., *Chem. Rev.* **1997**, *97*, 1647 – 1668; b) J. Rebek, Jr., *Acc. Chem. Res.* **1999**, *32*, 278 – 286.
[27] Organization of chromophoric dyes in polymer backbones has been shown to have a dramatic effect on their second-order nonlinear optical properties: a) W. Lin, W. Lin, G. K. Wong, T. J. Marks, *J. Am. Chem. Soc.* **1996**, *118*, 8034 – 8042; b) S. Di Bella, G. Lanza, I. Fragalà, S. Yitzchaik, M. A. Ratner, T. J. Marks, *J. Am. Chem. Soc.* **1997**, *119*, 3003 – 3006.
[28] C. A. Schalley, R. K. Castellano, M. S. Brody, D. M. Rudkevich, G. Siuzdak, J. Rebek, Jr., *J. Am. Chem. Soc.* **1999**, *121*, 4568 – 4579.

A Mixed-Valence and Mixed-Spin Molecular Magnetic Material: $[Mn^{II}L]_6[Mo^{III}(CN)_7][Mo^{IV}(CN)_8]_2 \cdot 19.5\,H_2O$**

Amandeep Kaur Sra, Marius Andruh, Olivier Kahn,* Stéphane Golhen, Lahcène Ouahab, and J. V. Yakhmi

The cyano bridge in an efficient and versatile magnetic coupler can mediate both antiferromagnetic and ferromagnetic interactions. This ability is the clue to the remarkable magnetic properties of bimetallic Prussian blue phases.[1–7] These phases can behave as ferrimagnets or ferromagnets with critical temperatures reaching 340 K. These phases, however, have some drawbacks. In particular, they have a faced-centered cubic structure,[8] so that no magnetic anisotropy can be expected. That is why we recently decided to use a heptacyanometalate, $[Mo(CN)_7]^{4-}$, instead of a hexacyanometalate as a precursor. The heptacoordination is not compatible with cubic symmetry. The reaction of $[Mo(CN)_7]^{4-}$ with Mn^{2+} ions afforded two- and three-dimensional compounds whose structures and magnetic properties were investigated in great detail.[9–12] As expected, the symmetries of the metal sites as well as the symmetry of the lattice as a whole are low, which leads to very interesting magnetic anisotropy properties.

[*] Prof. O. Kahn, A. Kaur Sra
Laboratoire des Sciences Moléculaires
Institut de Chimie de la Matière Condensée de Bordeaux
UPR CNRS No 9048
F-33608 Pessac (France)
Fax: (+33) 5-56-84-26-49
E-mail: kahn@icmcb.u-bordeaux.fr
Prof. M. Andruh
Inorganic Chemistry Laboratory
University of Bucharest, Chemistry Faculty
RO-70254 Bucharest (Romania)
Dr. S. Golhen, Dr. L. Ouahab
Laboratoire de Chimie du Solide et Inorganique Moléculaire
UMR CNRS No 6511
Université de Rennes 1, F-35042 Rennes (France)
Dr. J. V. Yakhmi
Chemistry Division, Bhabha Atomic Research Center
400085 Mumbai (India)

[**] This work funded by the Indo-French Centre for the Promotion of Advanced Research (IFCPAR, project no. 1308 – 4). L = 2,13-dimethyl-3,6,9,12,18-pentaazabicyclo[12.3.1]octadeca-1(18),2,12,14,16-pentaene.

  1433-7851/99/3817-2606 $ 17.50+.50/0

It occurred to us that the symmetry of the lattice could be lowered further by imposing heptacoordination not only to the Mo^{3+} sites but also to the Mn^{2+} sites. For that, we utilized the macrocycle 2,13-dimethyl-3,6,9,12,18-pentaazabicyclo-[12.3.1]octadeca-1(18),2,12,14,16-pentaene (L), which is known to adopt a planar conformation, which led to the stabilization of heptacoordinated Mn^{2+} species of the type $[MnL(H_2O)_2]^{2+}$ with a pentagonal-bipyramid geometry.[13, 14] The reaction of $[Mo(CN)_7]^{4-}$ with $[MnL(H_2O)_2]^{2+}$ afforded a compound of formula $[Mn^{II}L]_6[Mo^{III}(CN)_7][Mo^{IV}(CN)_8]_2 \cdot 19.5\,H_2O$ (**1**), whose structure and magnetic properties are reported here.

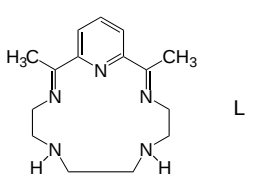

L

The structure of **1** contains five metal sites, namely, a molybdenum(III) site (Mo1), a molybdenum(IV) site (Mo2), and three manganese(II) sites (Mn1, Mn2, and Mn3). The organization is two-dimensional, and is made up of edge-sharing 48-membered rings (Figure 1). Each ring has a heart shape, and contains 16 metal sites: two Mo1 sites located on a twofold axis together with six Mo2, four Mn1, and four Mn3 sites in general positions. All these sites are linked by cyano bridges, the carbon atoms being bound to molybdenum and the nitrogen atoms to manganese. There are two kinds of linkages which are common to two adjacent rings, namely, Mo2-C-N-Mn3-N-C-Mo2 and Mo2-C-N-Mn1-N-C-Mo1-C-N-Mn1-N-C-Mo2. The Mn2 site is linked to the Mo2 site through a cyano bridge, but is not directly involved in the ring. The noncoordinated water molecules occupy the voids between the layers.

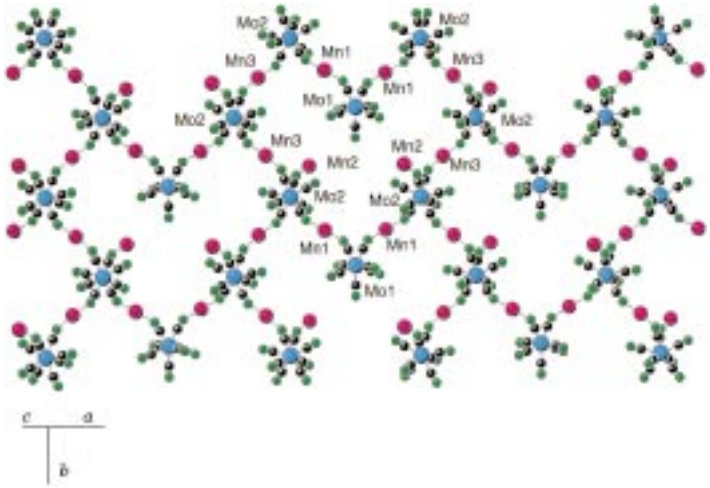

Figure 1. Structure of a layer of **1** consisting of edge-sharing heart-shaped 48-membered rings. For clarity, the macrocycles L have been omitted. Color code: molybdenum: blue, manganese: purple, carbon: black, nitrogen: green.

Let us now examine the environment of each molybdenum and manganese site. Site Mo1 is surrounded by two C-N-Mn1 linkages and five terminal cyano groups (Figure 2, left). The coordination sphere may be described as a distorted pentagonal bipyramid, with C12-N12 and $C12^{i}$-$N12^{i}$ along the pseudo fivefold axis. Site Mo2 is surrounded by one C-N-Mn1, one C-N-Mn2, and two C-N-Mn3 linkages together with four terminal cyano groups (Figure 2, right). The coordination has a low symmetry; however, it is reminiscent of a square antiprism.

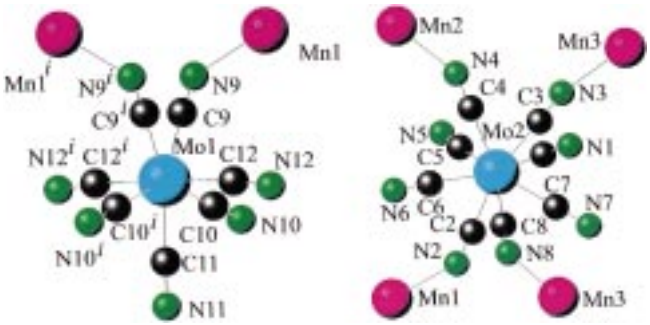

Figure 2. Environment of the Mo1 (left) and Mo2 sites (right) in **1**. The color code is the same as for Figure 1. Selected mean interatomic distances [Å] and angles [°]: Mo1–C 2.148, Mo2–C 2.166; Mo1-C-N 176.8, Mo2-C-N 176.8.

The three manganese sites are surrounded by the five nitrogen atoms of the macrocycle in the equatorial plane and two other coordinating atoms along the apical directions, leading to pentagonal-bipyramid geometries. Site Mn1 is bound to a N-C-Mo1 linkage along one of the apical directions, and a N-C-Mo2 linkage along the other (Figure 3, top). It is displaced from the mean plane defined by the five

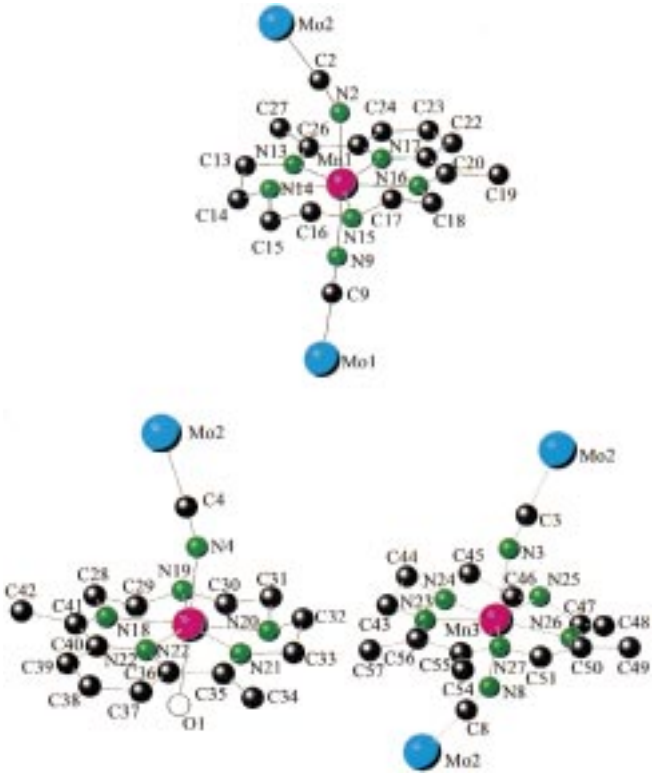

Figure 3. Environment of the Mn1 (top), Mn2 (bottom left; for reasons of clarity the purple sphere for Mn2 is not labeled), and Mn3 sites (bottom right) in **1**. The color code is the same as for Figure 1: the oxygen atom of the water molecule at Mn2 is represented by a white sphere. Selected interatomic distances [Å] and angles [°]: Mn1–N 2.281 (mean equatorial), Mn1–N2 2.324(9), Mn1–N9 2.282(8), Mn2–N 2.292 (mean equatorial), Mn2–N4 2.250(8), Mn2–O1 2.381(7), Mn3–N 2.285 (mean equatorial), Mn3–N3 2.283(9), Mn3–N8 2.316(9); Mn1-N2-C2 148.4(8), Mn1-N9-C9 142.9(8), Mn2-N4-C4 150.5(8), Mn3-N3-C3 146.6(9), Mn3-N8-C8 147.4(8).

  1433-7851/99/3817-2607 $ 17.50+.50/0

nitrogen atoms of the macrocycle by only 0.0208 Å. Site Mn2 is bound to a N-C-Mo2 linkage along one of the apical directions, and a water molecule along the other (Figure 3, bottom left). This site is pulled out of the mean plane defined by the five nitrogen atoms of the macrocycle toward the apical water molecule by 0.0931 Å. Site Mn3 (Figure 3, bottom right) has an environment close to that of Mn1. It is bound to two N-C-Mo2 linkages along the apical directions, and is displaced from the mean plane defined by the five nitrogen atoms of the macrocycle by 0.0172 Å.

The first striking result concerning the magnetic properties of **1** is the $\chi_M T$ value at room temperature of 10.8 emu K mol^{-1}, which is much lower than anticipated (χ_M = molar magnetic susceptibility, T = temperature). Let us examine the contributions of the different metal ions to this value. The Mo1 site is a low-spin Mo^{3+} ion with one unpaired electron;[15] its contribution to the high-temperature limit of $\chi_M T$ is close to 0.4 emu K mol^{-1}. The Mo2 site is a low-spin Mo^{4+} ion, with a diamagnetic local ground state. The Mn1, Mn2, and Mn3 sites can be either low-spin (LS) or high-spin (HS) Mn^{2+} ions. In the former case, the contribution is again close to 0.4 emu K mol^{-1}. In the latter case, the contribution is close to 4.4 emu K mol^{-1}.[16] Therefore, four out of six Mn^{2+} ions are LS, and the other two are HS. The Mn1 and Mn3 sites are close to each other, with two cyano ligands along the apical directions. On the other hand, the Mn2 site has only one cyano ligand occupying an apical position, together with a water molecule occupying the other apical position. Furthermore, the Mn2 site is pulled out from the equatorial plane, which diminishes the ligand field exerted by the macrocycle. There is no doubt that the field is stronger for the Mn1 and Mn3 sites than for the Mn2 site, and we will assign the LS local states to these sites. It follows that the local spins of the metal sites are $S_{Mo1} = 1/2$, $S_{Mo2} = 0$, $S_{Mn1} = S_{Mn3} = 1/2$, and $S_{Mn2} = 5/2$. The high-temperature limit of $\chi_M T$ is then expected to be close to 10.8 emu K mol^{-1}, which corresponds to the experimental value at room temperature.

As the temperature is lowered, $\chi_M T$ is first constant, then increases more and more rapidly, and reaches a maximum value of 18 emu K mol^{-1} around 4 K (Figure 4). Such behavior

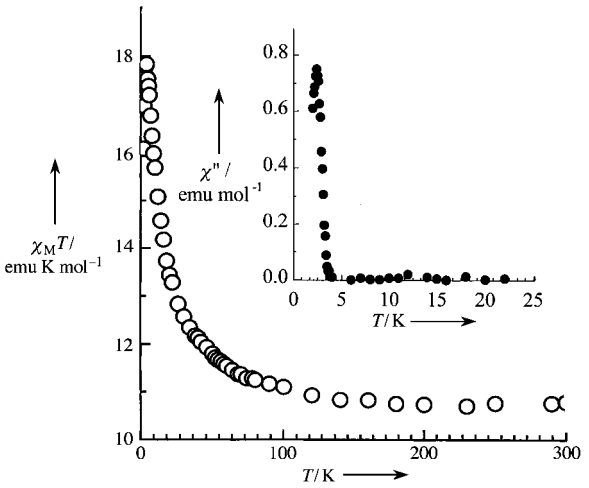

Figure 4. Plot of the temperature dependence of $\chi_M T$ for **1**. Inset: plot of the temperature dependence of the out-of-phase component of the ac magnetic susceptibility (χ'') under a zero static field.

reveals dominant ferromagnetic interactions between the spin carriers. The temperature dependences of the in-phase (χ') and out-of-phase components (χ'') of the molar magnetic susceptibility in the ac mode were also measured under a zero static field. As T is lowered, χ' increases continuously with an inflexion point around 3 K. The value of χ'' is zero down to 4 K, then presents a peak at 3 K, revealing a long-range ferromagnetic ordering (inset of Figure 4). The field dependence of the magnetization at 2 K is shown in Figure 5. No hysteresis was observed. Under 50 kOe, the magnetization is equal to 12.5 Nβ, while the saturation expected for 15 ferromagnetically coupled unpaired electrons is about 15 Nβ.

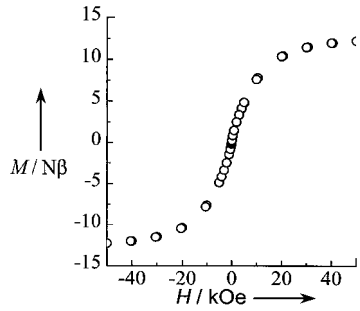

Figure 5. Plot of the field dependence of the magnetization for **1** at 2 K.

From a magnetic viewpoint, each heart-shaped ring involves ten local spins of 1/2 (S_{Mo1}, S_{Mn1}, and S_{Mn3}) and six diamagnetic Mo^{4+} sites. A local spin of 5/2 (S_{Mn2}) is attached to each of these Mo^{4+} sites. If the magnetic interactions were exclusively propagated through the cyano bridges, the magnetic topology would consist of Mn1-Mo1-Mn1 triads together with isolated Mn2 and Mn3 sites (see Figure 1). Such a topology has a magnetic dimensionality of zero, and cannot lead to a long-range magnetic ordering. Therefore, one must admit that some very weak interactions are also propagated through the closed-shell N-C-Mo2-C-N linkages, resulting in a magnetic dimensionality of two. Interlayer interactions and/or magnetic anisotropy permit the onset of a ferromagnetic transition around 3 K. What is remarkable is that all the interactions are ferromagnetic, through the cyano bridge as well as through the N-C-Mo2-C-N linkage.

The reaction of $[Mo^{III}(CN)_7]^{4-}$ with $[Mn^{II}L(H_2O)_2]^{2+}$ did not afford the expected compound of formula $[Mn^{II}L(H_2O)_2]_2[Mo^{III}(CN)_7] \cdot n H_2O$, but instead the title compound **1**, in which two thirds of the $[Mo^{III}(CN)_7]^{4-}$ groups have been oxidized to $[Mo^{IV}(CN)_8]^{4-}$ groups. No other compound could be detected in the solid state. The reaction was performed under strictly anaerobic conditions, so that $[Mo^{IV}(CN)_8]^{4-}$ probably arises from a partial disproportionation of $[Mo^{III}(CN)_7]^{4-}$, with Mo^{II} species remaining in solution.

Compound **1** may be considered as a fully localized mixed-valence species as well as a mixed-spin species. The $(MnL)^{2+}$ groups are involved in three different crystallographic sites. Two sites with two N-coordinated cyano groups along the apical directions have a LS state, and the site with one N-coordinated cyano group and one water molecule along the apical directions has a HS state.

The dominant interactions are ferromagnetic, and a long-range ferromagnetic ordering is observed at 3 K. The very low value of the critical temperature is due to the fact that the long-range ordering involves interactions not only through the cyano bridges, but through the N-C-Mo^{4+}-C-N bridging

  1433-7851/99/3817-2608 $ 17.50+.50/0

linkages as well. The latter are obviously very weak. Interestingly, the ferromagnetic interactions in Prussian blue also occur through the N-C-Fe^{2+}-C-N closed-shell linkage.[17–19]

Experimental Section

$K_4[Mo(CN)_7]\cdot 2H_2O$[15] and $[MnL(H_2O)_2]Cl_2\cdot 4H_2O$[14] were prepared as already described. Dark red single crystals of **1** were obtained by slow diffusion in an H-shaped tube under nitrogen of two deoxygenated 10^{-4} M aqueous solutions containing $K_4[Mo(CN)_7]\cdot 2H_2O$ and $[MnL(H_2O)_2]Cl_2\cdot 4H_2O$, respectively.

Crystal data for **1** ($C_{113}H_{126}N_{53}O_{19.5}Mn_6Mo_3$): monoclinic, space group $C2/c$; $a=40.30(3)$, $b=16.942(3)$, $c=24.464(13)$ Å; $\beta=120.98(2)^\circ$; $V=14319$ Å^3; $Z=4$. Data were collected on a four-circle diffractometer Enraf-Nonius with graphite-monochromated $Mo_{K\alpha}$ radiation. A total of 13592 reflections were collected in the range $1.18<\theta<25.46^\circ$, and were used after a semiempirical absorption correction had been applied. The structure was solved by direct methods and refined against all F^2 data to $R1=0.0714$, $wR2=0.1425$ for 5088 reflections with $I\le 2\sigma(I)$, GOF = 0.930. Crystallographic data (excluding structure factors) for the structure reported in this paper have been deposited with the Cambridge Crystallographic Data Centre as supplementary publication no. CCDC-117388. Copies of the data can be obtained free of charge on application to CCDC, 12 Union Road, Cambridge CB2 1EZ, UK (fax: (+44) 1223-336-033; e-mail: deposit@ccdc.cam.ac.uk).

The magnetic measurements were carried out with a Quantum Design MPMS-5S SQUID magnetometer working in both the dc and ac modes down to 2 K and up to 50 kOe. The diamagnetic correction was estimated as 1260×10^{-6} emu mol^{-1}.

Received: April 6, 1999 [Z13245IE]
German version: *Angew. Chem.* **1999**, *111*, 2768–2771

Keywords: cyano ligands · macrocyclic ligands · magnetic properties

[1] D. Babel, *Comments Inorg. Chem.* **1986**, *5*, 285.
[2] V. Gadet, T. Mallah, I. Castro, M. Verdaguer, *J. Am. Chem. Soc.* **1992**, *114*, 9213.
[3] T. Mallah, S. Thiebaut, M. Verdaguer, P. Veillet, *Science* **1993**, *262*, 1554.
[4] W. R. Entley, G. S. Girolami, *Inorg. Chem.* **1994**, *33*, 5165.
[5] W. R. Entley, G. S. Girolami, *Science* **1995**, *268*, 397.
[6] S. Ferlay, T. Mallah, R. Ouahès, P. Veillet, M. Verdaguer, *Nature* **1995**, *378*, 701.
[7] O. Kahn, *Nature* **1995**, *378*, 667.
[8] A. Ludi, H. Güdel, *Struct. Bonding (Berlin)* **1973**, *14*, 1.
[9] J. Larionova, J. Sanchiz, S. Golhen, L. Ouahab, O. Kahn, *Chem. Commun.* **1998**, 953.
[10] J. Larionova, R. Clérac, J. Sanchiz, O. Kahn, S. Golhen, L. Ouahab, *J. Am. Chem. Soc.* **1998**, *120*, 13088.
[11] J. Larionova, O. Kahn, S. Golhen, L. Ouahab, R. Clérac, *J. Am. Chem. Soc.* **1999**, *121*, 3349.
[12] O. Kahn, J. Larionova, L. Ouahab, *Chem. Commun.* **1999**, 945.
[13] M. G. B. Drew, A. H. bin Othman, *J. Chem. Soc. Dalton Trans.* **1997**, 438.
[14] O. Jiménez-Sandoval, D. Ramirez-Rosales, M. D. J. Rozales-Hoz, M. E. Sosa-Torres, R. Zamorano-Ulloa, *J. Chem. Soc. Dalton Trans.* **1998**, 1551.
[15] G. R. Rossman, F. D. Tsay, H. B. Gray, *Inorg. Chem.* **1973**, *12*, 824.
[16] O. Kahn, *Molecular Magnetism*, VCH, New York, **1993**.
[17] A. N. Holden, B. T. Mathias, P. W. Anderson, H. W. Lewis, *Phys. Rev.* **1956**, *102*, 1463.
[18] R. M. Bozorth, H. J. Williams, D. E. Walsh, *Phys. Rev.* **1956**, *103*, 572.
[19] N. Fukita, M. Ohba, H. Okawa, K. Matsuda, H. Iwamura, *Inorg. Chem.* **1998**, *37*, 842.

The Photoisomerization of *cis*-Stilbene Does Not Follow the Minimum Energy Path

Christian D. Berweger, Wilfred F. van Gunsteren,* and Florian Müller-Plathe

The development of femtosecond spectroscopy has made it possible to monitor chemical reactions in real time. As a prototype, the photoisomerization of stilbene in solvent has been examined under various conditions (temperature, pressure, solvent).[1–7] However, important issues such as the atomic detail of the reaction dynamics or the shape of the potential energy landscape still remain experimentally unresolved. Computational methods allow the detailed study of the time-resolved dynamics of these systems. Molecular dynamics[8, 9] provides the time-dependent evolution of the system and allows for effects due to temperature and solvent, whereas accurate potential energy surfaces are provided by quantum chemistry.[10] By combining the two methods,[11–14] the best from both worlds can be used: The explicit treatment of the solvent and the evolution in time by classical molecular dynamics, and the unbiased description of the reacting molecule by quantum chemistry. However, the latter is computationally rather demanding. Evaluation of potential energy and forces for photoexcited stilbene takes about half an hour on a modern microprocessor. As thousands, or rather millions of such evaluations are required for a meaningful molecular dynamics simulation, a straightforward implementation of this concept is not feasible. For this reason, we recently developed an interpolation method based on finite elements.[15, 16] The method represents the part of the potential energy surface that is required during the simulation without losing the accuracy of the quantum chemical method. This reduces the number of quantum chemical evaluations by a factor of about 2000 compared to a straightforward implementation. However, only the central dihedral angle and the two phenyl torsion angles are allowed to move for the method to be efficient. Also, the model does not include deactivation mechanisms such as fluorescence or internal conversion.

Stilbene in its first excited state is treated by a singly excited configuration interaction calculation in a 6-31G basis set. Supercritical argon is used as a model solvent at the appropriate density (2744 argon atoms with periodic boundary conditions, Lennard-Jones parameters for classical solvent–solvent and stilbene–solvent interaction from the GROMOS96 force field[9]). In total, 800 trajectories were simulated at different pressures and temperatures, at least 20 trajectories for a single state point. More computational details are given elsewhere.[16] Previous theoretical work on

[*] Prof. Dr. W. F. van Gunsteren, Dipl.-Chem. C. D. Berweger
Laboratorium für Physikalische Chemie
Eidgenössische Technische Hochschule Zürich
CH-8092 Zürich (Switzerland)
Fax: (+41) 1-632-1039
E-mail: wfvgn@igc.phys.chem.ethz.ch
Priv.-Doz. Dr. F. Müller-Plathe
Max-Planck-Institut für Polymerforschung
D-55128 Mainz (Germany)

  1433-7851/99/3817-2609 $ 17.50+.50/0